AIMS Materials Science, 12(1): 55–67.
DOI: 10.3934/matersci.2025005
Received: 29 August 2024
Revised: 10 January 2025
Accepted: 17 January 2025
Published: 22 January 2025

http://www.aimspress.com/journal/Materials

Research article

Luminescence modification of porous silicon decorated with GOQDs synthesized by green chemistry

Francisco Severiano Carrillo[1,2,*], Orlando Zaca Moran[2,*], Fernando Díaz Monge[3,*] and Alejandro Rodríguez Juárez[3]

[1] CONAHCYT, Av. Insurgentes Sur 1582, Col. Crédito Constructor, Del. Benito Juárez C.P. 03940, Ciudad de México
[2] Centro de Investigación en Biotecnología Aplicada Unidad Tlaxcala, Instituto Politécnico Nacional, Carretera a Santa Inés Tecuexcomac, a 1.5 km, Ex-Hacienda San Juan Molino, C.P. 90700, Tlaxcala, México
[3] Tecnológico Nacional de México, ITS-Tlaxco. Predio Cristo Rey Ex-Hacienda de Xalostoc. Carretera Apizaco-Tlaxco Km. 16.8. C.P. 90271, Tlaxco, Tlaxcala

* **Correspondence:** Email: fseveriano@secihti.mx; balarama_1@yahoo.com.mx; ozacam@ipn.mx; fernando.dm@tlaxco.tecnm.mx; Tel: 5-557-296-000.

Abstract: In this work, the luminescent emission control from porous silicon (PS) decorated with graphene oxide quantum dots (GOQDs) was analyzed. The samples obtained showed a 95 nm range of variation in which the luminescent emission can be controlled. Based on the results obtained from the PS samples decorated with GOQDs, the emission can be selected in a range from blue to red. Fourier transform infrared (FTIR) spectroscopy showed evidence of bond formation between PS and GOQDs. These changes can be related to the changes in luminescent emission. Photoluminescence analysis showed that the main PS emission can be selected in a 90 nm range with the introduction of GOQDs. Scanning electron microscopy (SEM) images and energy dispersive spectroscopy (EDS) spectra demonstrated the introduction of GOQDs in the PS. X-ray diffraction patterns also confirmed the presence of GOQDs on the surface of PS. In this study, different methodologies to control the luminescent emission were applied, and the results show that PS samples decorated with GOQDs showing blue, orange, and red luminescence can be obtained. The samples obtained can be applied to the development of electroluminescence devices, photodetectors, and biosensors.

Keywords: porous silicon; GOQDs; luminescent; green-synthesized; nanostructures

1. Introduction

Porous silicon (PS) is a material with a huge range of applications due to its physicochemical properties, which can assist in the development of devices like sensors [1], combustible cells [2], and light sources [3], among others. Among its primary properties are an efficient photoluminescence at room temperature [4] and its high surface reactivity due to its great effective area [5]. These properties can be controlled by the pore size and the porous layer thickness. Techniques such as electrochemical etching (one of the main techniques to obtain PS) can easily control these parameters by changing the etching time, the electrolyte, and the type of silicon wafer used. As such, PS samples can be used with the characteristics needed to develop biosensors or electroluminescence devices. However, to develop some devices, the inherent properties of PS layers can be a problem. For example, the quenching of the luminescent emission (due to oxidation) for its high reactivity, as well as the increase of resistivity of the porous layer, can make it challenging to develop electroluminescent devices. Because of this, it is necessary to search for solutions that allow the implementation of PS samples in the generation of new technologies. A possible solution is the addition of materials in the porous structure, which must improve PS properties. For example, to build biosensors, a functionalization process is applied to prepare the porous layer for the introduction of biological materials. Another example is the introduction of a material with luminescent emission in the PS structure to help with the construction of a luminescent device.

Graphene oxide quantum dots (GOQDs) are serious competitors to semiconductor-based quantum dots (QDs), due to their similar physical properties but superior chemical properties, namely high biocompatibility, low toxicity, and easy manufacturing and functionalization. In recent years, QDs have played a fundamental role in biotechnological development, with more effective properties due to their high porosity, lighter weight with high performance, being composed of many π bonds and oxygen groups [6], functional groups C–O, C=O, COOH, as well as sp^2 and sp^3 hybridizations [7]. Such properties have been of great interest in research topics such as optoelectronics, sensing, or bioimaging diagnostics [8]. Currently, the use of carbon nanoparticles is centered on the development of simple, efficient, and economical production technologies. Different synthesis methods have been implemented, such as laser ablation or cathodic arc discharge; these processes require high energy consumption and high cost [9]. Within these synthesis methods, exfoliation, a carbon-based nanostructure synthesis technique that is cheap and easy to implement, was found to aid in the development of friendly materials, while protecting the environment and population health. This concern has directed the search for other alternatives for the manufacture of biofunctional nanostructures, avoiding harmful reagents or chemical processes potentially dangerous for the environment. Zero-dimensional carbon-based nanomaterials such as GOQDs present a fascinating quasispherical morphology with less than 10 nm diameters, with a wide variety of interesting bioapplications such as photoluminescence [10]. Due to its quantum confinement and edge effects, which can be explained by electron-hole recombination occurring after the excitation of electrons by an external energy source, this photoluminescence is of great interest [11,12].

In this work, the luminescent emission of PS when GOQDs were introduced in its porous structure, after being obtained via green synthesis, was analyzed. The photoluminescent characterization shows

that the luminescent emission can be altered by the introduction of the GOQDs in the PS structure; additionally, the importance of the heat treatment in this change was demonstrated. The photoluminescence can be controlled in a 95 nm range. The morphological characterization was obtained by scanning electron microscopy (SEM). The morphologic analysis shows the formation of a layer of GOQDs over the PS surface. Energy-dispersive X-ray spectroscopy (EDS) microanalysis confirms the introduction of GOQDs in the PS structure. The Fourier transform infrared spectroscopy (FTIR) characterization demonstrated that the oxidation and inclusion of GOQDs modify the chemical properties of the PS. Finally, X-ray diffraction (XRD) patterns also confirm the introduction of carbon in the surface of PS.

2. Materials and methods

2.1. Obtaining PS

To obtain the PS samples, P-type boron doped crystalline silicon (c-Si) with direction (100), 230–250 μm thickness, and 8–12 Ωcm resistivity was used. Samples were obtained by electrochemical etching in a Teflon cell. A tungsten cathode was used, and the c-Si worked as the anode. The electrolyte used was a mixture of hydrofluoric acid (HF) and ethanol (C_2H_6O) in a proportion of 1:2. The current used was 1 mA and the etching time was 30 min.

2.2. Green-synthesized GOQDs from orange peel

The orange peel was washed with deionized water and then dehydrated. A furnace Barnstead Thermolyne 1000 was used with a heating ramp of 5 °C/min until reaching 1100 °C; a cylindrical stainless steel 316 reactor with a 5 mL/min flow of nitrogen was used for the carbonization of the orange peel. The carbon was placed in isopropyl alcohol (Sigma-Aldrich) and then in an ultrasonic bath (Branson 3800) for 90 min for the exfoliation process. Afterward, the solution was centrifuged at 15,000 rpm (Science MED Finland Technology D2012) for 5 min to obtain GOQDs. GOQDs were prepared at a ratio of 2.3 μg of GOQDs per 1 mL of isopropyl alcohol, in a total 100 μL solution. For each process, deposition was at a rate of 5 μL every 2 min. The ultrasonic bath and spin coating process was repeated 20 times.

2.3. Experimental process

Figure 1 shows the process by which PS samples were decorated with 100 μL of GOQDs. Each sample had two characterization processes, as indicated in the labels. Samples (a) and (c) were subjected to two heat treatment (Ht) processes. Ht was performed at 180 °C for 12 h. In the case of the ultrasonic treatment (Ut), 100 μL was introduced with the help of a micropipette in 20 steps of 5 μL each. After each 5 μL step, the sample was introduced in the ultrasonic machine for 1 min. When spin coating was used, 100 μL of GOQDs was added to the samples in 20 steps of 5 μL. After each 5 μL step, a spin process (Sp) at 3000 rpm for 1 min was applied to the sample.

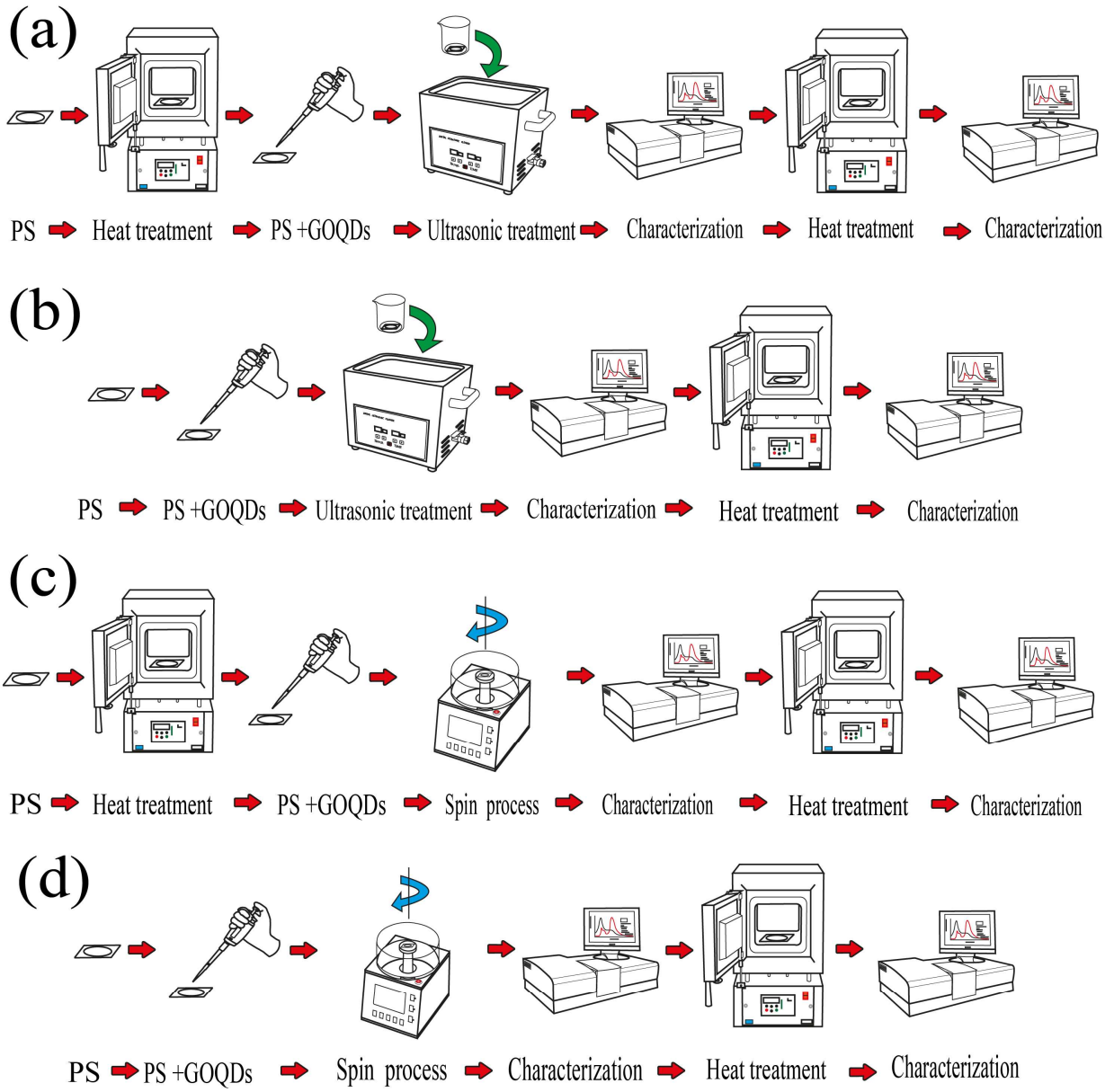

Figure 1. Methodology of the different PS samples decorated with GOQDs. (a) and (b) ultrasonic treatment. (c) and (d) spin coating.

2.4. Characterization

Optical absorption spectra of GOQD colloid dispersions were recorded using a UV-Vis-NIR scanning spectrophotometer (Thermo Scientific, Evolution 600 model). The structural characterization of GOQDs was made by transmission electron microscopy (TEM) in a Tecnai G2 T20 TEM operating at 300 kV. The morphologic characterization was performed using an electronic microscope Tescan Vega TS 5136SB with a resolution of 3 nm; secondary and backscattered electrons detectors were used. Chemical composition was analyzed by EDS, performed on a Jeol JSM-IT300 electron microscope. A Rigaku Ultima IV diffractometer with a Cu-Kα (1.54 Å) radiation source was used for the morphologic characterization. A Vertex 70 Bruker spectrometer was used to obtain the FTIR spectrum in attenuated

total reflection (ATR) mode with a range of 4000–400 cm^{-1}. Changes in the luminescent emission were analyzed with a spectrometer (Ocean Optics, USB4000 model). To obtain photoluminescent spectra, samples were excited with a 405 nm LED source (Ocean Insight, model L405A).

3. Results and discussion

3.1. UV-Vis spectroscopy and fluorescence of GOQDs

UV-Vis spectroscopy of GOQDs shows characteristic C–C bonds (π–π*) at 220 nm, C=C bonds (π–π*) at 270 nm, and C=O bonds (n–π) at 330 nm. In Figure 2a, the size of the GOQDs obtained by TEM microscopy is presented with sizes of 3 nm [13,14]. In Figure 2b, the fluorescence emission of the GOQDs excited at 350 nm is shown, with an emission energy of 2.8 eV associated with the characteristic blue emission of the GOQDs [13,14].

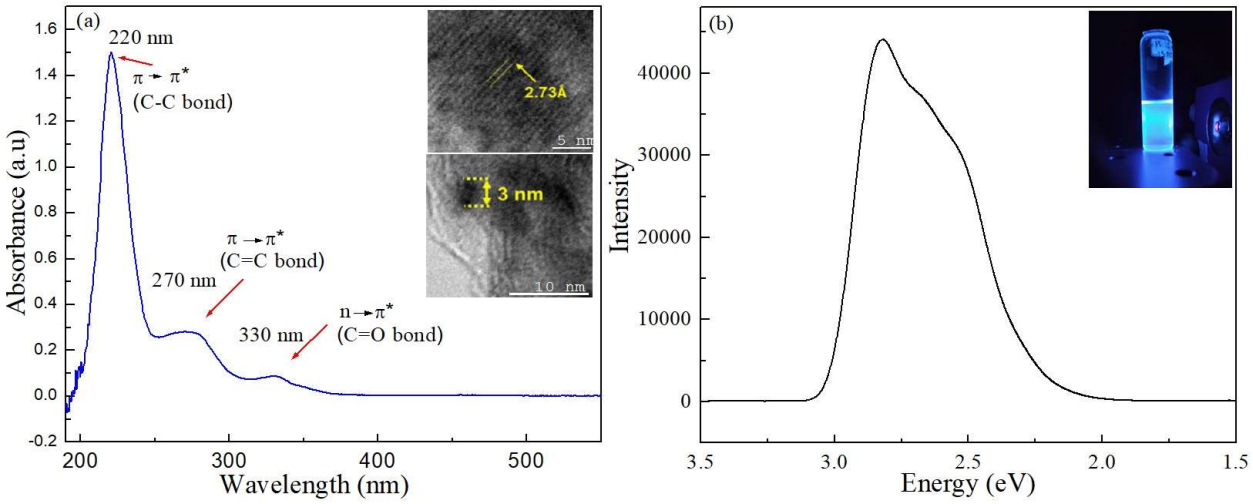

Figure 2. GOQDs spectra. (a) UV-Vis and TEM; (b) fluorescence and blue emission characteristic of the GOQDs excited with a 350 nm lamp.

3.2. Photographs of the luminescent emission

Figure 3 shows the photographs taken from the PS samples decorated with GOQDs, in which the photoluminescence in each characterization can be appreciated. The samples with Ht previous to the first characterization show poor luminescence (Figure 3a,c) and a major contribution of the GOQDs (blue tone). This supports the idea that GOQDs have a screening effect over the luminescent PS. Besides, the Ht reduces the contribution from GOQDs.

Luminescent intensities show a relationship with the photoluminescence spectra. Samples without Ht (Figure 3b,d) show a major contribution of the PS in the total luminescence. This can be due to the lack of Ht. Also, the contribution of the GOQDs as blue stains can be appreciated. These samples show a relationship between the luminescent intensity and the spectra. Finally, after all the different processes, samples show a homogenous orange luminescence. This can be due to the change in the emission of the GOQDs, which change to longer wavelengths after Ht [14]. The contribution of both emissions (PS and GOQDs) can be observed in the increment of the intensity in the photoluminescence.

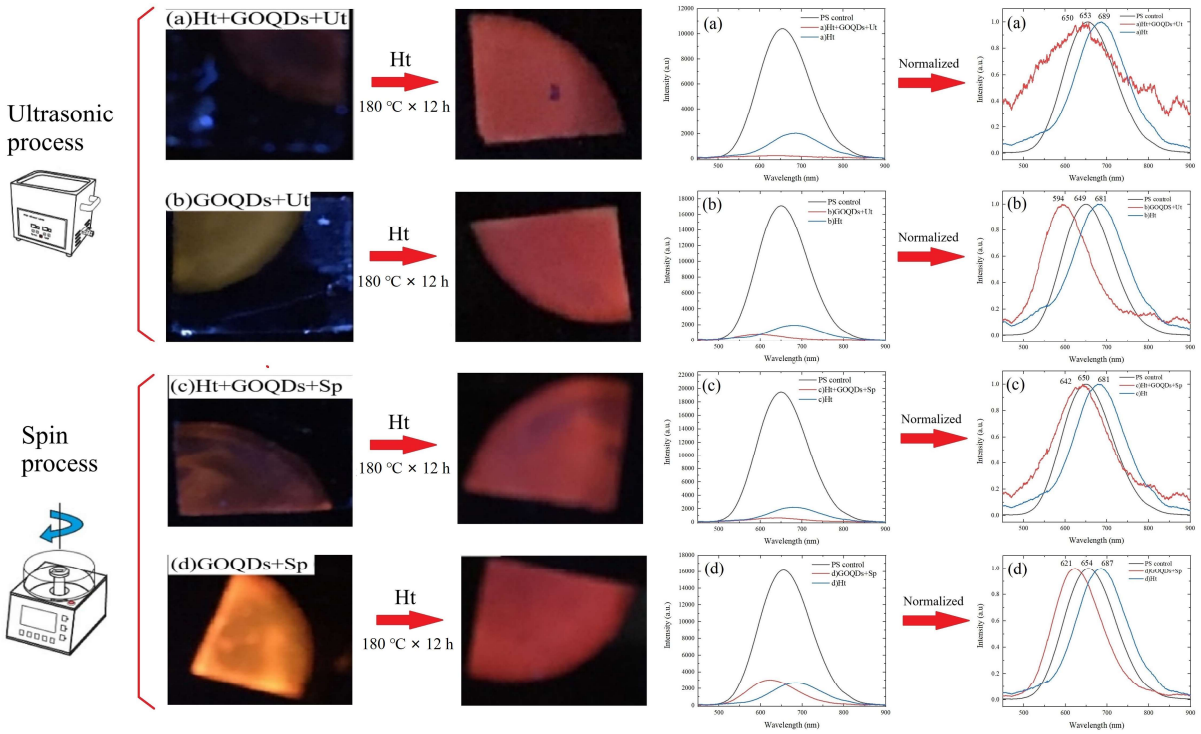

Figure 3. Photographs and photoluminescence spectra of PS samples during the different processes, showing the changes in the luminescent emission with the introduction of GOQDs in the PS with two decoration processes. Process 1: ultrasonic treatment. (a) Ht + GOQDs + Ut with Ht. Photoluminescence spectra from the samples of PS, Ht + GOQDs + Ht. (b) GOQDs + Ut with Ht. Photoluminescence spectra from the samples of PS, Ht + GOQDs + Ht. Process 2: spin coating. (c) Ht + GOQDs + Sp with Ht. Photoluminescence spectra from the samples of PS, Ht + GOQDs + Ht. (d) GOQDs + Sp with Ht. Photoluminescence spectra from the samples of PS, Ht+ GOQDs+Ht. All spectra were normalized.

Photoluminescence spectra are also shown in Figure 3, after the image of luminescence emission from PS and the PS/GOQDs. Samples with Ht previous to the first characterization show an important reduction of the luminescence intensity and a light shift to short wavelengths (Figure 3a,c). The reduction in intensity is mainly due to the Ht, as it is well-known that this effect is generated by the oxidation in the silicon nanocrystals in which the luminescent emission takes place [15]. Oxidation introduces non-recombinative centers that generate luminescence quenching; this also generates a size reduction of the silicon nanocrystals, changing their emission wavelength, which explains the observed shift to short wavelengths [16]. The reduction in intensity can also be due to a screening effect from the GOQDs. Another explanation for the shift to short wavelengths can be attributed to the luminescence of the GOQDs since this is their region of emission [17]. This analysis can also be applied to the samples obtained with spin and ultrasonic processes. For the samples without Ht, in their first characterization, a reduction in luminescence intensity is also observable, besides an important shift to short wavelengths, as can be seen in Figure 3b,d. In these samples, the loss of intensity of the luminescence can be attributed to the screening effect. Since these samples do not have Ht, and the

reduction effect is observed, the shift to short wavelengths can be mainly due to the GOQDs since they cover the PS surface and their emission predominates.

Previous to the second characterization, an Ht was performed for all samples. An increment in the luminescent intensity is seen in Figure 3a–c but not in sample (d), which shows a minimum reduction; also, all samples show a shift to long wavelengths. The increment of the luminescent emission is due to the change of the maximum of the GOQDs, which change after a Ht to longer wavelengths [7,18,19]. They also show the spectra of luminescence with a normalization process to better observe the changes to the samples during the experiments. In Figure 3, it can be observed that the samples with one Ht show a range of about 90 nm in which the luminescent emission can be controlled. The emission of samples with two heat treatments shows a range of 40 nm in which emission can be controlled. The spectra of all samples show a shift to short wavelengths in the first part of the study (samples with Ht before the first characterization). It is very likely that the emission of the GOQDs is the most predominant since they are over the PS surface. For the second part of the study (Ht before the second characterization), a shift to long wavelengths can be clearly observed, likely due to the combination of the photoluminescence of PS and GOQDs, since after a Ht, GOQDs show a shift to long wavelengths. It is seen that the Ht in the PS and GOQDs modifies their principal emissions; then, it is possible to control the wavelength of emission of PS with the introduction of GOQDs in their structure and the use of heat treatments. To control emission, GOQDs could be introduced in the PS surface, and the desired wavelength can be obtained by applying Ht to select the principal emission. We normalized the photoluminescence of PS samples decorated with GOQDs to better observe such shifts in photoluminescence (last graphs of Figure 3).

3.3. PS/ GOQDs SEM and EDS analysis

Figure 4 shows the morphological characterization obtained by SEM. In this image, the surfaces of PS and PS/GOQDs are shown. The sample label "control" shows PS without GOQDs in its structure, in which the size of the pore is around 0.693 ± 0.021 μm. Figure 4 shows the surfaces of the PS/GOQDs samples after the final step. There is a visible formation of a GOQD film over the surface of the PS. Also, cluster formation can be observed. This demonstrates that the screening effect described before is possible. The insets show zones of the samples in which the GOQD film is broken and the surface of the PS can be observed.

In Table 1, the pore size of the PS samples is summarized. The sizes of the pores are characteristics of these kinds of samples.

Table 1. Pore size of the PS used to introduce GOQDs in their structure.

Sample	Control	A	B	C	D
Pore size mean (μm)	0.693 ± 0.021	0.711 ± 0.023	0.741 ± 0.28	0.544 ± 0.017	0.785 ± 0.026

Table 2 shows the values obtained by EDS analysis. This characterization confirms the presence of GOQDs on the PS surface. The samples obtained with Ut show a major concentration of GOQDs. This can be related to photoluminescence intensity since these samples show minor emission when compared with the samples obtained with Sp. However, samples obtained with Sp show similar shifts in the maximum of the luminescent emission.

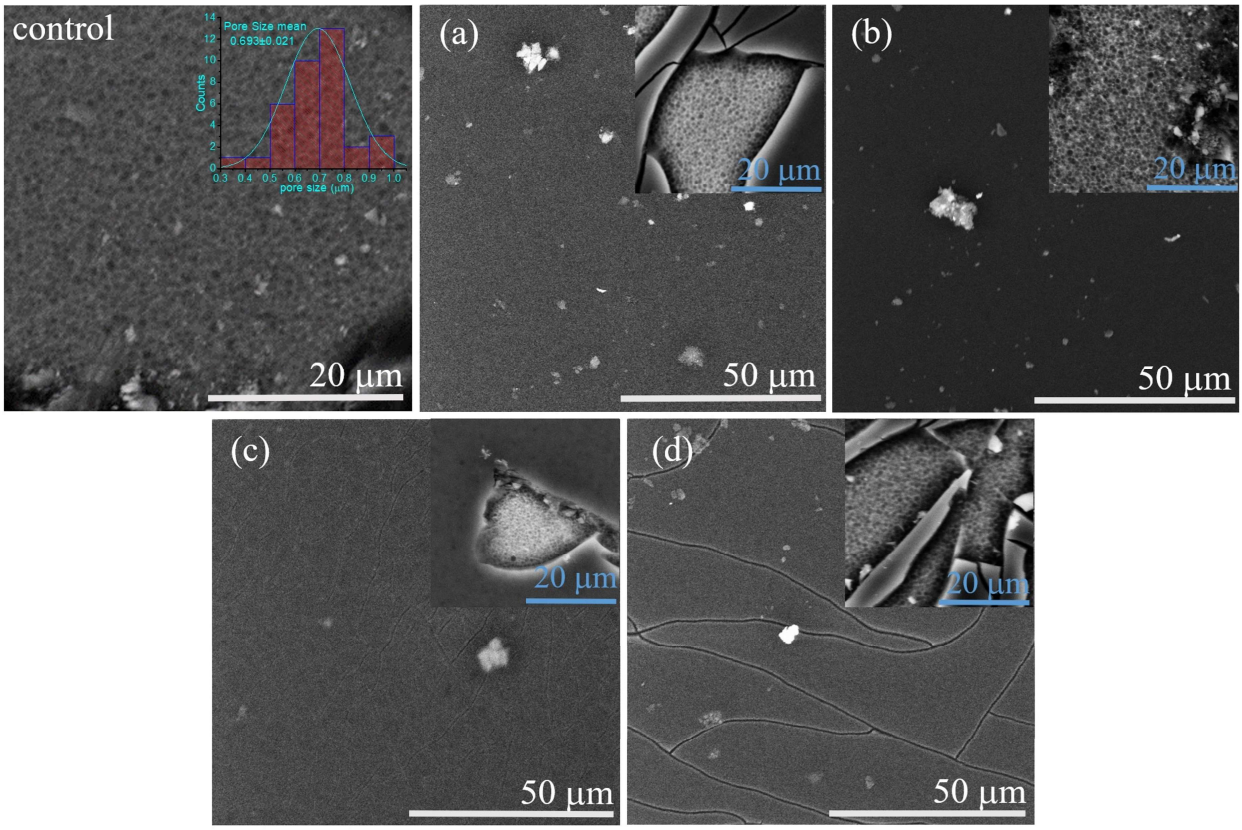

Figure 4. SEM micrographs of (control) PS without GOQDS, (a) PS with heat treatment and GOQDs deposited via ultrasonic bath, (b) PS without heat treatment with GOQDs deposited via ultrasonic bath, (c) PS with heat treatment and GOQDs deposited via spin coating, and (d) PS without heat treatment and GOQDs deposited via spin coating. All samples were heat-treated once GOQDs were deposited.

Table 2. EDS analysis of the PS/GOQDs samples, in which the quantity of carbon on the surface can be observed.

Sample	Carbon (%)	Oxygen (%)	Silicon (%)
1 (a)	25.23	39.82	34.95
2 (b)	50.55	26.33	23.11
3 (c)	28.36	38.15	33.49
4 (d)	3.48	51.40	45.12

3.4. XRD analysis

Figure 5A shows the XRD spectrum of the graphite obtained from orange peel. In this spectrum, peaks 24 and 44° are observed to be related to the graphite (JCPDS Card Files, No. 41-1487). This sample was characterized in powder form, so the peaks observed between 30 and 40° correspond to the sample holder and are not observed in the PS/GOQDs samples [20]. Figure 5B shows the XRD spectrum of the PS/GOQDs sample. The results show peaks associated with GOQDs at 24 and 44°, which correspond to GOQDs. This analysis confirms the introduction of GOQDs into porous

silicon [21]. Peaks associated with the PS are not observed; this can be due to the formation of the GOQDs film that covers the surface of the PS.

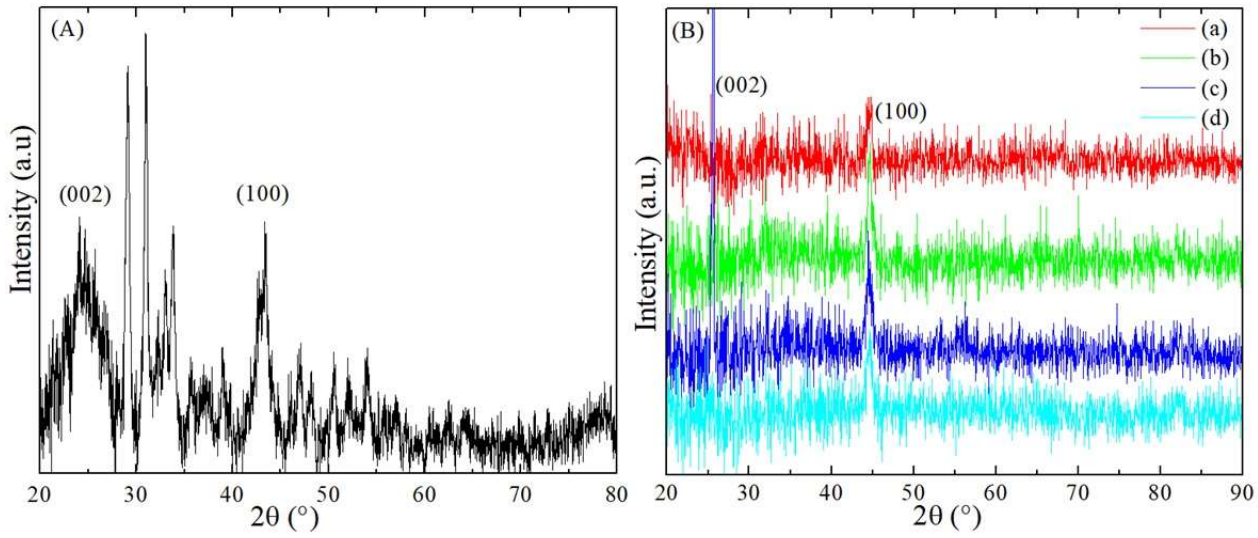

Figure 5. (A) Diffractogram of graphite oxide obtained from orange peel, (B) where the sample (a) corresponds to PS with heat treatment and GOQDs deposited via an ultrasonic bath, (b) corresponds to PS without heat treatment with GOQDs deposited via an ultrasonic bath, (c) PS with heat treatment and GOQDs deposited via spin coating, and (d) PS without heat treatment and GOQDs deposited via spin coating. All samples were heat treated once the GOQDs were deposited.

3.5. FTIR analysis

Figure 6 shows the IR spectra obtained from PS and PS/GOQDs. Four regions of interest show vibrational changes. The band related to Si–Si and Si–H was found between 545 and 690 cm^{-1} [22]; it is important to note that this band reduces its intensity due to the formation of Si–C bonds formed during the Ht process. This result is supported by the band related to the formation of Si–C bonds. The band at 690–819 cm^{-1} [23] is related to the absorption of Si–C bonds; this is not present in the spectrum related to the PS, as it is due to the inclusion of the GOQDs. The band between 854 and 894 cm^{-1} is due to the O_nSiH_x deformation in the PS surface [24]; this band shows an increment in intensity when the Ht is applied to the PS samples decorated with GOQDs. The final region of interest is around 2057–2387 cm^{-1}, related to the Si–H absorption bands [25]; this band shows a reduction in intensity when the Ht is performed. This suggests that during this process, bonds between PS and GOQDs occur. The IR characterization demonstrated that the oxidation and the inclusion of GOQDs modify the chemical properties of the PS. These changes in the samples modify the luminescent characteristics. The changes in the emission of PS are generated by changes in the lattice in the PS network once GOQDs and oxide layers are introduced in their structure.

The ultrasonic treatment showed better results as samples presented signals from 594 to 689 nm, with a shift of 95 nm; on the other hand, the PS samples with spin coating treatment showed a variation from 621 to 687 nm, with a variation of 66 nm. As supported by these results, the ultrasonic process is the method that allows a wider range.

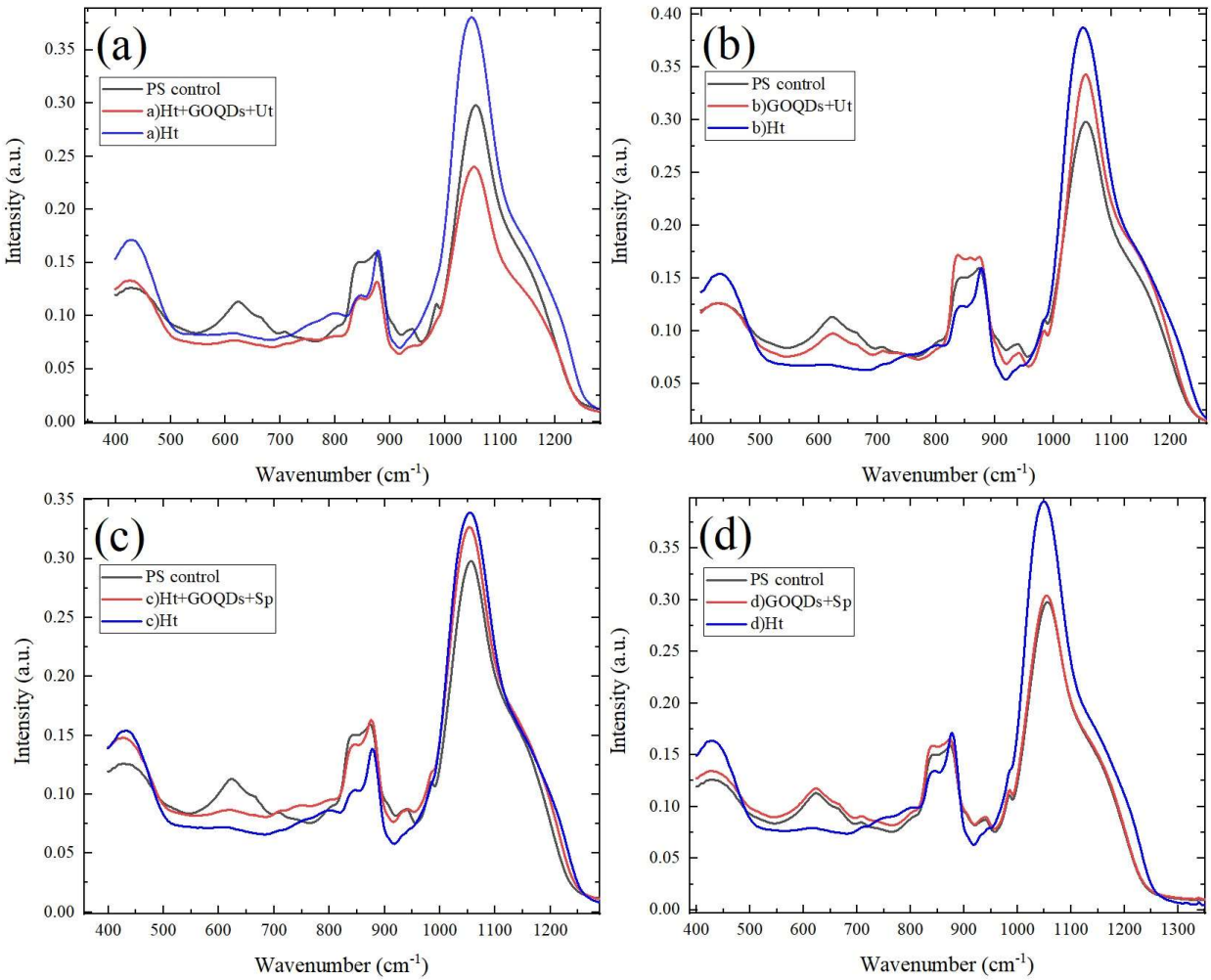

Figure 6. FTIR spectra of PS, according to the process with and without heat treatment after decoration with GOQDs. (a) and (b) PS with and without heat treatment with GOQDs deposited via ultrasonic bath; (c) and (d) PS with and without heat treatment with GOQDs deposited via spin coating.

4. Conclusions

This work shows that the luminescent emission of PS can be modified with the introduction of GOQDs in the porous structure. Photoluminescence results showed that the main emission of PS can be selected in a range between 594 and 689 nm with the introduction of GOQDs. SEM images demonstrated that the GOQDs form a film over the PS. EDS spectra and XRD patterns confirm the presence of GOQDs in the PS. FTIR spectroscopy shows evidence of the formation of bonds between silicon and GOQDs. In this study, two methods to control luminescent emission were analyzed; results demonstrated that blue, orange, and red luminescent emission can be obtained. Samples obtained can be applied to the development of electroluminescence devices, photodetectors, and biosensors.

Use of AI tools declaration

The authors declare they have not used Artificial Intelligence (AI) tools in the creation of this article.

Acknowledgments

F. Severiano thanks CONAHCYT for its support through project 165 of cátedras CONAHCYT, Project supported by CONAHCYT in 2023 with number CF-2023-G-1080 and to the Instituto Politecnico Nacional, through financing SIP 20240719. The project was partially supported by TecNM in 2024 with project number: 20228.24-PD.

Author contributions

F. Severiano and O. Zaca prepared the experiments and wrote the main manuscript text. F. Díaz Monge and A. Rodríguez Juárez helped with the analysis and with the redaction of text.

Data availability

The data that support the findings of this study are available from the corresponding author upon reasonable request.

Conflict of interest

The authors declare no conflict of interest.

References

1. Vercauteren R, Leprince A, Mahillon J, et al. (2021) Porous silicon biosensor for the detection of bacteria through their lysate. *Biosensors* 11: 27. https://doi.org/10.3390/bios11020027
2. Gör Bölen M, Karacali T (2020) A novel proton-exchange porous silicon membrane production method for μDMFCs. *Turk J Chem* 44: 1216–1226. https://doi.org/10.3906/kim-2002-32
3. Fauchet PM (1998) The integration of nanoscale porous silicon light emitters: materials science, properties, and integration with electronic circuitry. *J Lumin* 80: 53–64. https://doi.org/10.1016/S0022-2313(98)00070-2
4. Robbiano V, Paternò GM, La Mattina AA, et al. (2018) Room-temperature low-threshold lasing from monolithically integrated nanostructured porous silicon hybrid microcavities. *ACS Nano* 12: 4536–4544. https://doi.org/10.1021/acsnano.8b00875
5. Riikonen J, Salomäki M, van Wonderen J, et al. (2012) Surface chemistry, reactivity, and pore structure of porous silicon oxidized by various methods. *Langmuir* 28: 10573–10583. https://doi.org/10.1021/la301642w
6. Chen Z, Wang M, Fadhil AA, et al. (2021) Preparation, characterization, and corrosion inhibition performance of graphene oxide quantum dots for Q235 steel in 1 M hydrochloric acid solution. *Colloids Surf A Physicochem Eng* 627: 127209. https://doi.org/10.1016/j.colsurfa.2021.127209

7. Xiao X, Zhang Y, Zho L, et al. (2022) Photoluminescence and fluorescence quenching of graphene oxide: A review. *Nanomaterials* 12: 2444. https://doi.org/10.3390/nano12142444
8. Zhang J, Zhang X, Bi S (2022) Two-dimensional quantum dot-based electrochemical biosensors. *Biosensors* 12: 254. https://doi.org/10.3390/bios12040254
9. Hossain MA, Islam S (2013) Synthesis of carbon nanoparticles from kerosene and their characterization by SEM/EDX, XRD and FTIR. *J Nanosci Nanotechnol* 1: 52–56. https://doi.org/10.11648/j.nano.20130102.12
10. Huang S, Yang E, Liu Y, et al. (2018) Low-temperature rapid synthesis of nitrogen and phosphorusdual-doped carbon dots for multicolor cellular imaging and hemoglobin probing in human blood. *Sens Actuators B Chem* 265: 326–334. https://doi.org/10.1016/j.snb.2018.03.056
11. Kurniawan D, Chen YY, Sharma N, et al. (2022) Graphene quantum dot-enabled nanocomposites as luminescence and surface-enhanced Raman scattering biosensors. *Chemosensors* 2022: 10. https://doi.org/10.3390/chemosensors10120498
12. Xu Q, Gong Y, Zhang Z, et al. (2019) Preparation of graphene oxide quantum dots from waste toner, and their application to a fluorometric DNA hybridization assay. *Mikrochim Acta* 186: 483. https://doi.org/10.1007/s00604-019-3539-x
13. Zaca-Moran O, Sánchez-Ramírez JF, Herrera-Pérez JL, et al. (2021) Electrospun polyacrylonitrile nanofibers as graphene oxide quantum dot precursors with improved photoluminescent properties. *Mater Sci Semicond Process* 127: 105729. https://doi.org/10.1016/j.mssp.2021.105729
14. Sengottuvelu D, Shaik AK, Mishra S, et al. (2022) Multicolor nitrogen-doped carbon quantum dots for environment dependent emission tuning. *ACS Omega* 7: 27742−27754. https://doi.org/10.1021/acsomega.2c03912
15. Kayahan E (2011) The role of surface oxidation on luminescence degradation of porous silicon. *Appl Surf Sci* 257: 4311−4316. https://doi.org/10.1016/j.apsusc.2010.12.045
16. Carrillo FS, Arcila-Lozano L, Salazar-Villanueva M, et al. (2023) Porous silicon used for the determination of bacteria concentration based on its metabolic activity. *Silicon* 15: 6113–6119. https://doi.org/10.1007/s12633-023-02502-7
17. Sun Z, Li X, Wu Y, et al. (2018) Origin of green luminescence in carbon quantum dots: specific emission bands originate from oxidized carbon groups. *New J Chem* 42: 4603. https://doi.org/10.1039/c7nj04562j
18. Correcher V, Garcia-Guinea J, Delgado A (2000) Influence of preheating treatment on the luminescence properties of adularia feldspar ($KAlSi_3O_8$). *Radiat Meas* 32: 709–715. https://doi.org/10.1016/S1350-4487(00)00121-9
19. Jiang W, Wang S, Li Z, et al. (2021) Luminescence spectra of reduced graphene oxide obtained by different initial heat treatments under microwave irradiation. *Diam Relat Mater* 116: 108388. https://doi.org/10.1016/j.diamond.2021.108388
20. Lou Z, Huang H, Li M, et al. (2014) Controlled synthesis of carbon nanoparticles in a supercritical carbon disulfide system. *Materials* 7: 97–105. https://doi.org/10.3390/ma7010097
21. Huang Y, Luo J, Peng J, et al. (2020) Porous silicon-graphene-carbon composite as high performance anode material for lithium ion batteries. *J Energy Storage* 27: 101075. https://doi.org/10.1016/j.est.2019.101075
22. Nayfeh M, Rigakis N, Yamani Z (1997) Photoexcitation of Si-Si surface states in nanocrystallites. *Phys Rev B Condens Matter* 56: 2079–2084. https://doi.org/10.1103/PhysRevB.56.2079

23. Basak FK, Kayahan E (2022) White, blue and cyan luminescence from thermally oxidized porous silicon coated by green synthesized carbon nanostructures. *Opt Mater* 124: 111990. https://doi.org/10.1016/j.optmat.2022.111990
24. Gupta P, Dillon A, Bracker AS, et al. (1991) FTIR studies of H_2O and D_2O decomposition on porous silicon surfaces. *Surf Sci* 245: 360–372. https://doi.org/10.1016/0039-6028(91)90038-T
25. Ogata Y, Niki H, Sakka T (1995) Oxidation of porous silicon under water-vapor environment. *J Electrochem Soc* 142: 1595–1601. https://doi.org/10.1149/1.2048619

AIMS Press